The International Journal of Advanced Manufacturing Technology (2018) 96:1483–1496
https://doi.org/10.1007/s00170-018-1722-6

ORIGINAL ARTICLE

Investigation on initial grain size and laser power density effects in laser shock bulging of copper foil

Chao Zheng[1] · Xiu Zhang[1] · Zheng Liu[1] · Zhong Ji[1] · Xiao Yu[2] · Libin Song[1]

Received: 24 August 2017 / Accepted: 5 February 2018 / Published online: 13 February 2018

Abstract
Laser shock bulging process is a promising flexible microforming method in which the laser shock wave pressure is employed to cause plastic deformation and fabricate microfeatures on thin sheet metals. However, the influence of initial grain size and laser power density on the forming quality of bulged parts has not been well understood. In this paper, three various initial grain sizes as well as three levels of laser power densities were provided, and then, laser shock bulging experiments of T2 copper foil were conducted. The characteristics of bulging height, thickness distribution, microhardness, surface morphology, and microstructure were examined. It is revealed that the bulging height increases with the increase of grain size and the enhancement of laser power density. The exhibiting good formability of pure copper foil in laser shock bulging process is attributed to the inertial effect on necking stabilization and strain-rate effect on material constitutive behavior. The overall thickness of bulged parts decreases compared with its original thickness. Moreover, the microhardness in the laser-shocked region increases due to the strain hardening effect, but the microhardness distribution is nonuniform because of the inhomogeneous plastic deformation. The grain sizes of bulged parts are slightly refined with the increase of laser power density, especially for the coarse-grained part. The grain refinement in laser shock bulging forming process is attributed to the large plastic deformation at high strain rates under laser shock.

Keywords Laser shock bulging · Grain size effect · Microforming · Laser forming · Forming quality analysis

1 Introduction

With the dramatic development of micro-electromechanical system (MEMS), many novel manufacturing technologies for products with feature dimensions in millimeter and submillimeter ranges have been proposed during recent years, and show their notable advantages in the field of MEMS. Microforming process, which fabricates parts via plastic deformation, has got tremendous attention for its high productivity, near net shape, high material usage, and low cost [1]. In the conventional microforming process, the metallic punch and die are adopted to form parts. Usually, both the punch and die need to be changed while a part with various geometry or sizes is formed. In addition, the technical challenges, such as the guarantee of the punch/die clearance and precision fabrication of micropunch, are still required for further study. Thus, using a flexible tool instead of the metal punch, known as the flexible forming method, offers attractive characteristics of excellent flexibility and high efficiency. One of the promising flexible microforming approaches is laser shock bulging process, in which a high-power laser pulse is utilized to generate shock wave pressure and the induced pressure can subsequently make the metal target plastically deform at high strain rates. The working principle of the process is illustrated in Fig. 1. In order to generate the plasma followed by the shock wave, the power density of the laser pulse is generally up to GW/cm^2 order. Compared with laser welding and laser cutting processes, the high-amplitude shock wave pressure rather than heat energy is employed to cause plastic deformation during laser shock bulging. Therefore, the process is nonthermal, which is beneficial for the mechanical property of microparts [2]. Over the years, the researches focus on the

✉ Libin Song
derby@sdu.edu.cn

[1] Key Laboratory for Liquid-Solid Structural Evolution and Processing of Materials Ministry of Education, School of Materials Science and Engineering, Shandong University, 17923 Jingshi Road, Jinan 250061, People's Republic of China

[2] State Grid Jinan Changqing Power Supply Company, 15508 Jingshi West Road, Jinan 250399, People's Republic of China

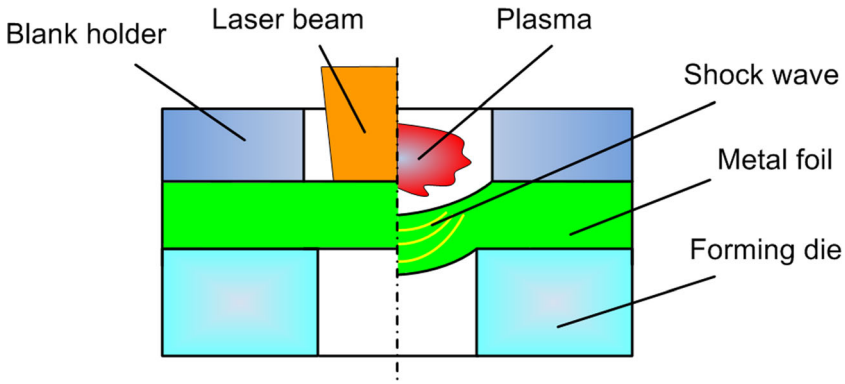

Fig. 1 Working principle of laser shock bulging process

forming mechanism [3–5] and laser and die critical parameters [6], the acting pressure during bulging [7], effect of confining overlay [8], and forming method assisted by polyurethane rubber [9]. It is proved that the laser shock bulging process has been successfully applied to form the common metallic materials such as copper, aluminum, and stainless steel.

It is well known that while the feature dimension of microparts is reduced from macroscale to microscale, the plastic deformation behavior of the material is generally determined by a few grains located in the deformation zone. Then, both the mechanical property and deformation behavior of the material are significantly different from those in the macroscale due to the so-called size effects [10]. Vollertsen et al. [11] gave a systematic review on size effects and their influence on micromanufacturing processes. Over the past decades, the grain size effect has been found to have a significant impact on microforming processes in terms of deformation behavior and product quality. Raulea et al. [12] employed bending experiments on thin aluminum sheet to study the grain size effect on mechanical properties of the material. They found that the yield strength declines with the increasing grain size attributed to the well-known Hall-Petch relationship. Gau et al. [13] carried out three-point bending experiments to investigate the influence of the ratio of foil thickness to grain size on springback behavior of brass in microbending process. They concluded that the springback amount of brass foil can be expressed as a function of the ratio when the foil thickness is less than 350 μm. Kim et al. [14] analyzed the effects of feature size, grain size, foil thickness, and preform shape on the forming of microfeatures by using microcoining process. Justinger et al. [15] attempted to understand the grain size and grain orientation effects by using a mathematic model considering the number of grains. Hmida et al. [16] investigated the initial grain size effect on the forming force evolution in microscale single point incremental forming process. The experimental results show that the drop of forming force with respect to the grain size is in connection with the Hall-Petch relationship. Ghassemali et al. [17] examined the interactive effect of grain size and sheet thickness on the material flow and microstructure evolution in a progressive open-die microforming process. Wang et al. [18] conducted experimental studies on the influence of grain size on flow-induced defects in microextrusion process of pure copper. The results show that for fine grains, the microparts have good flow lines in consistent with part shape, while for coarse grains, there are no obvious flow lines due to only several grains located in the deformation region. Gao et al. [19] revealed the grain size effect on the plastic deformation of pure copper in roll-to-plate micro/meso-imprinting process by experiments and numerical simulations. Fu et al. [20] focused on the grain size effect on microscale blanking and deep drawing compound process of copper sheet. They found that the plastic deformation becomes inhomogeneous with the increase of grain size and the decrease of formed part size, resulting in the irregular geometry and rough surface morphology of microparts. Xu et al. [21] explored the grain size effect on the deformation behavior of brass foil via microblanking experiments. They concluded that the deformation behavior of the material depends on the blanking clearance as well as the initial grain size. Meng et al. [22] systematically discussed the interactive effects of grain size, lubrication condition, and tool velocity on deformation behavior, section quality, and dimensional accuracy for both the blanked part and the pierced hole. It is revealed that the forming quality is declined with the increase of grain size and tool velocity.

Based on the above brief review of the studies on grain size effect, it can be seen that the experimental and numerical investigations are mainly concentrated in microforming processes under quasi-static loading conditions. However, less effort has been made in grain size effect under high strain rate loading conditions, especially induced by pulsed laser shock loading. Hu et al. [23] investigated the grain size effect on the microindentation depth of pure copper generated by laser shock. It is concluded that the microindentation depth strongly relates to the initial grain size. Wang et al. [24] explored size effects on the deformation behavior of copper foil in microscale laser bending process. They found that both the ratio of foil thickness to grain size and the ratio of microchannel dimension to foil thickness have significant influence on the forming amount and the surface morphology. However, the

grain size effect on other basic forming processes induced by laser shock, especially for bulging forming, has not been well understood. In this sense, it is full of the importance to explore the grain size effect on plastic deformation and forming quality of metal foil in laser shock bulging process.

It is obvious that the laser power density plays an important role in the interaction of laser pulse with metal foil. In our prior study, the effect of laser power density on forming height, residual stress distribution, and surface morphology of the absorbent coating has been investigated [25]. However, the influence of laser power density on the forming quality of bulged parts, characteristics of thickness distribution, microhardness, and microstructure is still not well understood. In this study, the ratio of foil thickness to initial grain size was adopted to represent the relationship of foil thickness and grain size. Three various initial grain sizes as well as three levels of laser power densities were provided, and then laser shock bulging experiments of pure copper foil were conducted. Based upon the experimental results, the effects of initial grain size and laser power density on the forming quality of bulged parts were discussed via the evaluation of bulging height, thickness distribution, microhardness, surface morphology, and microstructure.

2 Experiments

2.1 Experimental setup

The experimental assembly of laser shock bulging process is shown in Fig. 2. The fundamental mechanism and critical processing components can refer to our prior work [3]. In particular, the black paint and quartz glass are two indispensable components for realization of the process. The black paint acts as an absorbent coating and interacts with the pulsed laser to generate high-temperature and high-pressure plasma. It has been proved that the absorbent coating can efficiently protect the metal foil from laser ablation. The application of quartz glass as a confining overlay can magnify the amplitude of shock wave pressure up to gigapascal levels compared with that in the open-air condition. Due to the ultrashort interaction time, the metal foil is plastically deformed at high strain rates while the pressure exceeds the dynamic yield strength of the material.

In the experiments, a Q-switched Nd:YAG laser system with a Gaussian spatial distribution beam was employed. The laser wavelength is 1064 nm, and the pulse duration is around 8 ns. All of the experiments were implemented by a single laser pulse. Laser drilling process was used to fabricate through holes in a stainless steel sheet as forming dies. Before laser shock, one surface of metal foil was carefully sprayed with black paint. The detailed experimental parameters are listed in Table 1. After bulging forming, the remaining black paint on the foil surface was removed using acetone solution for 20 min in an ultrasonic cleaner, and then, anhydrous alcohol was adopted to clean the foil surface.

After laser shock bulging experiments, the surface morphology of bulged parts was observed through scanning electron microscopy (JSM-6610LV). The dimensions of parts were measured by video measuring system (VMS-4030F). The height of the highest position of the dome-like shape, defined as the maximum bulging height, is adopted to represent the deformation degree, as shown in Fig. 3. The specimens were then cut through the highest position of parts, and the cross section was used to analyze the thickness distribution, microhardness, and microstructure of bulged parts. The load of 10 g was applied on the cross section for 15 s to achieve the microhardness by Vickers hardness test (HV-1000).

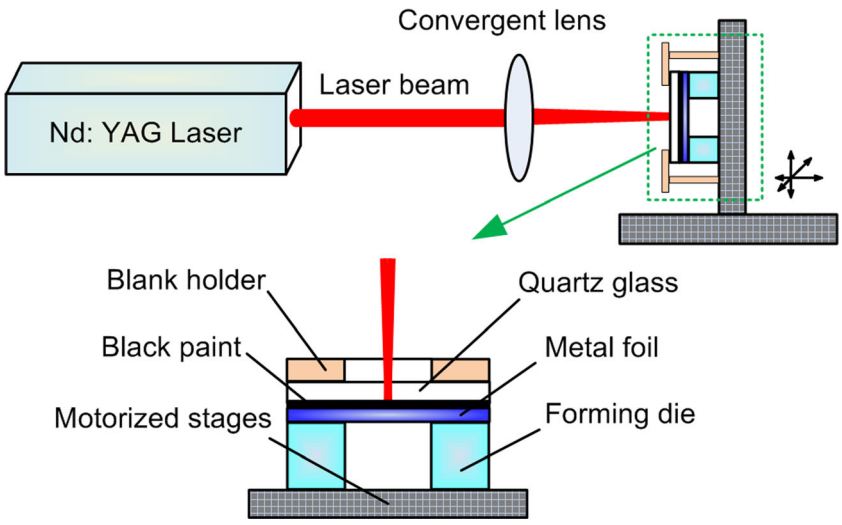

Fig. 2 Experimental assembly of laser shock bulging process

Table 1 Detailed experimental parameters

Parameters	Laser beam diameter (mm)	Die hole diameter (mm)	Quartz glass thickness (mm)	Black paint thickness (μm)	Laser power density ($\times 10^{13}$ W/m^2)
Value	2	1.4	2	~50	2.63, 3.07, 3.51

2.2 Specimen preparation

The material chosen for the experimental investigation is T2 pure copper foil of 50 μm in thickness (t) due to its wide application in the field of MEMS. The as-received copper foils were annealed in a vacuum furnace at the temperatures of 450, 600, and 750 °C for 1 h to obtain various initial grain sizes (d). In order to protect the ultrathin metal foil from destruction by the conventional hot mounting method, the metallographic specimens were prepared using the cold mounting method. The bulged parts were placed in a mounting cup, and then, the mixture of epoxy resins and hardener was poured into the cup followed by curing. After carefully grinding and polishing, the specimens were etched with a $FeCl_3$ (5 g) + HCl (15 ml) + H_2O (100 ml) solution for 15~20 s. Then, the average grain size in the thickness direction was measured by the mean linear intercept method according to the ASTM E112 standard. The microstructures of annealed foils in the cross section of thickness are shown in Fig. 4. The ratio of foil thickness to initial grain size ($N = t/d$) was adopted to represent the relationship of foil thickness and grain size. The obtained grain sizes and the corresponding N values are listed in Table 2.

3 Results and discussion

3.1 Bulging height

Figure 5 presents deformation values of copper foils with various grain sizes and laser power densities. Five specimens were tested in each condition, and the standard deviation was calculated. Based upon the measurements, it is manifest that under all of the applied laser power densities, considerable plastic deformation occurs without failure for all N values. Furthermore, as the laser power density is enhanced, the maximum bulging height with various N values exhibits the same growth trend. In the case of $N = 1.3$, the maximum bulging height even increases from 251.3 μm (2.63×10^{13} W/m^2) to 344.3 μm (3.51×10^{13} W/m^2). Thus, it implies that the laser power density is one of the critical processing parameters for the plastic deformation induced by laser shock. Due to the fact that the interaction of laser and material significantly depends on the laser power density, it is important to be clear about the magnitude of generated shock wave pressure.

For the case that the laser shock process is implemented in the confining regime, the relationship between the peak shock wave pressure and the laser power density can be expressed as follows [26]:

$$P_{\max} = 10^{-9}\sqrt{\left(\frac{\alpha}{2\alpha+3}\right)\cdot Z\cdot I_0} \quad (1)$$

where $P_{\max}$ is the peak shock wave pressure induced by the laser pulse, α is the fraction of the internal energy devoted to

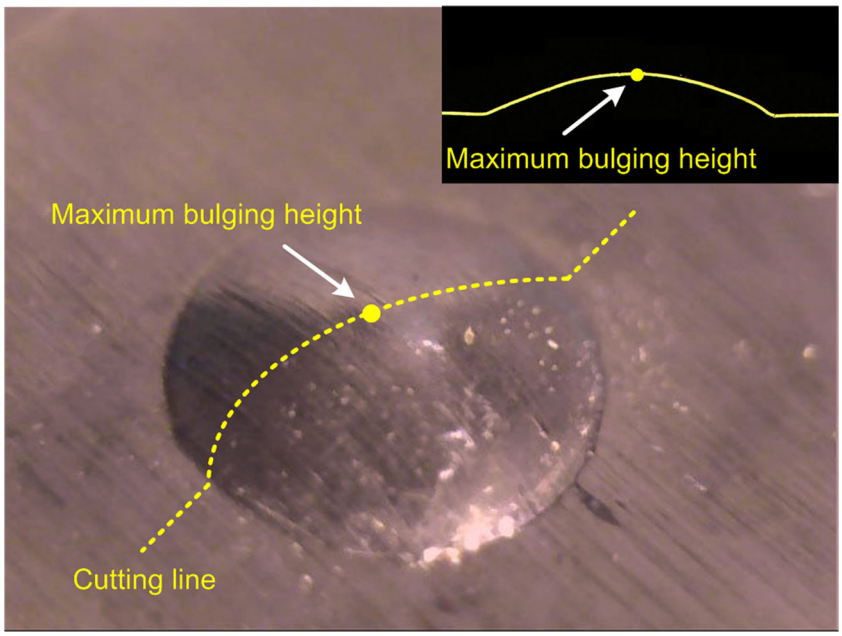

Fig. 3 Preparation of specimens for microscopic analysis

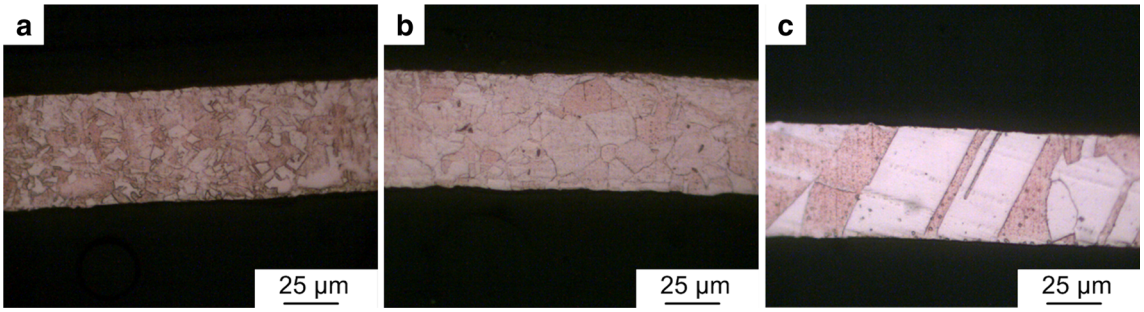

Fig. 4 Microstructures of copper foil after heat treatment. **a** 450 °C, 1 h. **b** 600 °C, 1 h. **c** 750 °C, 1 h

the thermal energy (generally equal to 0.1), I_0 is the laser power density, and Z is the shock impedance which can be given by the relation:

$$\frac{2}{Z} = \frac{1}{Z_{\text{metal}}} + \frac{1}{Z_{\text{overlay}}} \tag{2}$$

where Z_{metal} and Z_{overlay} are the impedance of the metal foil (T2 copper) and the confining overlay (quartz glass), and are 3.83×10^7 and 1.31×10^7 kg/m^2 s, respectively [25]. Thus, the peak pressure calculated from the above model is 4.01, 4.33, and 4.63 GPa corresponding to the laser power density of 2.63×10^{13}, 3.07×10^{13}, and 3.51×10^{13} W/m^2, respectively. Obviously, the higher laser power density can magnify the amplitude of shock wave pressure, indicating that larger plastic deformation can be achieved. However, it is noted that the laser power density should not be too high to avoid the occurrence of fracture. Figure 6 presents a fractured part at $N = 4.0$ and 3.94×10^{13} W/m^2. For the reason that the tensile strength limit of metal foil at ultrahigh strain rates is difficult to examine, the applied laser power density is often repeatedly tested to achieve an appropriate value for specific material. In this study, the laser power density range of 2.63×10^{13} to 3.51×10^{13} W/m^2 can induce considerable plastic deformation without failure for 50-μm pure copper foil.

Moreover, under the same level of laser power density, it can be clearly seen that the maximum bulging height increases gradually as N value diminishes, as shown in Fig. 5. In other words, it means that the larger maximum bulging height can be achieved through enlarging the initial grain size. This trend is similar to that in microforming processes under quasi-static loading conditions since the flow stress of materials decreases with the increase in grain size according to the empirical Hall-Petch relationship [11]. At $N = 1.3$, the grain size increases to the same order of the foil thickness. In this case, the mechanical properties of the individual grains will dominate the properties of the foil. While the grain orientation is unfavorable towards the bulging direction, it may result in an adverse effect on the development of plastic deformation. However, according to Fig. 5, the foil with coarse grains exhibits large plastic deformation, indicating that the laser power density is a key factor to affect the bulging height of metal foil.

A remarkable phenomenon in laser shock bulging process is that the average bulging height can reach 344.3 μm for copper foil with 50 μm in thickness at $N = 1.3$ and 3.51×10^{13} W/m^2. In magnetic pulse forming [27] and electrohydraulic forming processes [28], the experimental results also show that the sheet metals have good formability at high strain rates. Neugebauer et al. [29] conducted a comprehensive review on velocity effects in metal forming and machining processes. They pointed out that the high forming velocity indeed helps to expand the limits of material formability and achieve complex-shaped products. Therefore, the large bulging height in laser shock bulging process is attributed to (1) inertial effect on necking stabilization. When the metal foil is impacted by a nanosecond laser pulse, the strain rate can reach 10^5–10^7 s^{-1} relying on the applied laser power density and pulse duration [30]. At such high strain rates, the inertia effect cannot be neglected and deeply affects the neck growth. During the bulging process, the inertial force can diffuse deformation throughout the metal foil, resulting in stabilizing the development of neck in local regions. (2) Strain-rate effect on material constitutive behavior. The flow stress and strain-rate sensitivity become significant while the strain rate is greater than 10^3 s^{-1} [31]. This effect also affects the deformation behavior of metal foil during laser shock bulging process.

Table 2 Heat treatment parameters and the corresponding grain sizes

Annealing process	450 °C, 1 h	600 °C, 1 h	750 °C, 1 h
Grain size (μm)	12.6	23.1	37.1
N	4.0	2.2	1.3

3.2 Thickness distribution

In order to examine the characteristics of thickness distribution of bulged parts, 31 points were selected in the cross section and an interval of 50 μm between points was adopted. Their positions can be seen in Fig. 7. Points 2 and 30 are located at the fillet region of the part, and point 16 is at the bottom.

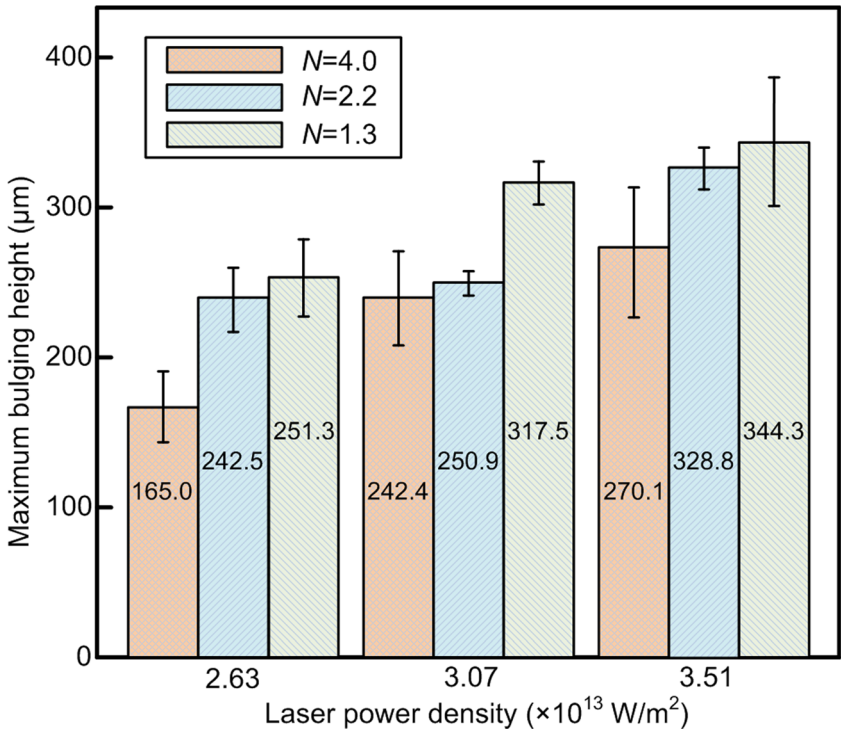

Fig. 5 Influence of initial grain size and laser power density on maximum bulging height of bulged parts

Figure 8 presents the typical thicknesses distribution with three N values under 2.63×10^{13} W/m^2. It can be seen that the measured thickness distribution is nonuniform due to the inhomogeneous deformation in the cross section. In addition, it is observed that the overall thickness of bulged parts decreases compared with its original thickness 50 μm. This means that the whole material within the die hole has been plastically deformed. Furthermore, it is noted that the location of the thinnest position is mainly in the fillet region of parts, indicating that the material of the corresponding region undergoes extensive plastic deformation during laser shock.

As the laser power density is enhanced up to 3.51×10^{13} W/m^2, the typical thicknesses distribution with three N values is shown in Fig. 9. Obviously, the overall thickness of bulged parts also decreases and the thinnest position is at the fillet region. However, the thickness at the fillet region under 3.51×10^{13} W/m^2 (35.41 μm at $N = 1.3$) is smaller than that under 2.63×10^{13} W/m^2 (44.02 μm at $N = 1.3$). This change implies that larger plastic deformation occurs with the enhancement of laser power density.

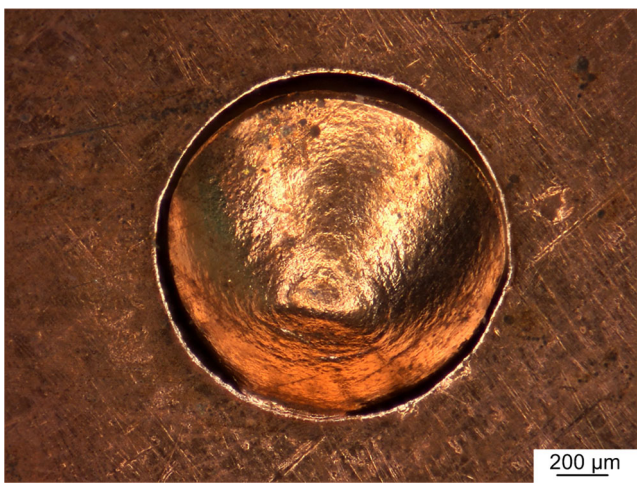

Fig. 6 Fractured part at $N = 4.0$ and 3.94×10^{13} W/m^2

In order to further investigate the thickness thinning of bulged parts, the maximum thickness thinning ratio R is defined as:

$$R = \frac{t_{\text{original}} - t_{\text{thinnest}}}{t_{\text{original}}} \times 100\% \quad (3)$$

where t_{original} is the original thickness of metal foil (50 μm) and t_{thinnest} is the minimum thickness of bulged parts. Then, the maximum thickness thinning ratio with various grain sizes and laser power densities is calculated and listed in Table 3. It is noted that although the thickness reduction at $N = 1.3$ and 3.51×10^{13} W/m^2 approaches 29%, the bulged part still maintains integrity without fracture and presents good formability.

As seen in Figs. 8 and 9, the maximum thickness thinning ratio appears at the fillet region of bulged parts. This phenomenon is related to the stress and strain characteristics during laser shock bulging. Figure 10 presents the force acting of metal foil during laser shock bulging process. The material in the deformation zone suffers from laser shock pressure, clamping force from blank holder and forming die, and pressure from die corner at the entrance. Due to the fact that the material out of the die hole is clamped by the blank holder, it is

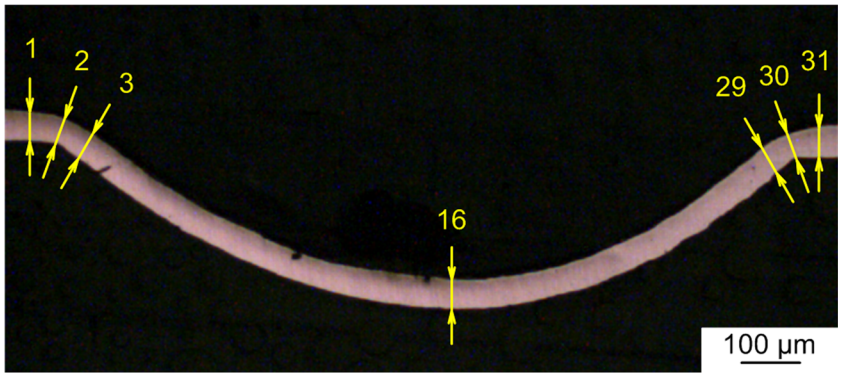

Fig. 7 Key thickness measurements of bulged parts

difficult to flow into the die hole. Thus, the plastic deformation of the material is realized by the reduction in thickness and the elongation along in-plane directions, resulting in the decrease of the overall thickness of bulged parts. Moreover, the material located at the fillet region suffers the pressure from the small radius of the die corner, leading to the extensive plastic deformation due to the die geometry. Thus, the maximum thickness thinning is inclined to appear in this region.

3.3 Microhardness

Hardness test is commonly used to evaluate the mechanical property of the part, and the hardness distribution can evaluate the plastic deformation of formed metal [19]. Thus, the Vickers hardness measurement was taken to analyze the mechanical property of metal foil after laser shock bulging forming. Figure 11 shows the measured positions in the cross section of bulged parts. Seven indentations were conducted, and an interval of 350 μm between measured points was adopted. Three specimens were tested in each condition. For the reason that the laser beam diameter in the experiments was 2 mm, points a and g are on the outside of the laser-shocked region and can be used to represent the initial hardness of metal foil. Points b and f are located at the fillet region of the part, and point d is at the bottom.

Figure 12 reveals the microhardness distribution in the cross section of bulged parts with three N values under 2.63×10^{13} W/m^2. Compared with those in the unshocked region, it can be clear to see that the microhardness in the laser-shocked region increases due to the strain hardening effect. However, the measured microhardness distribution is nonuniform because of the inhomogeneous plastic

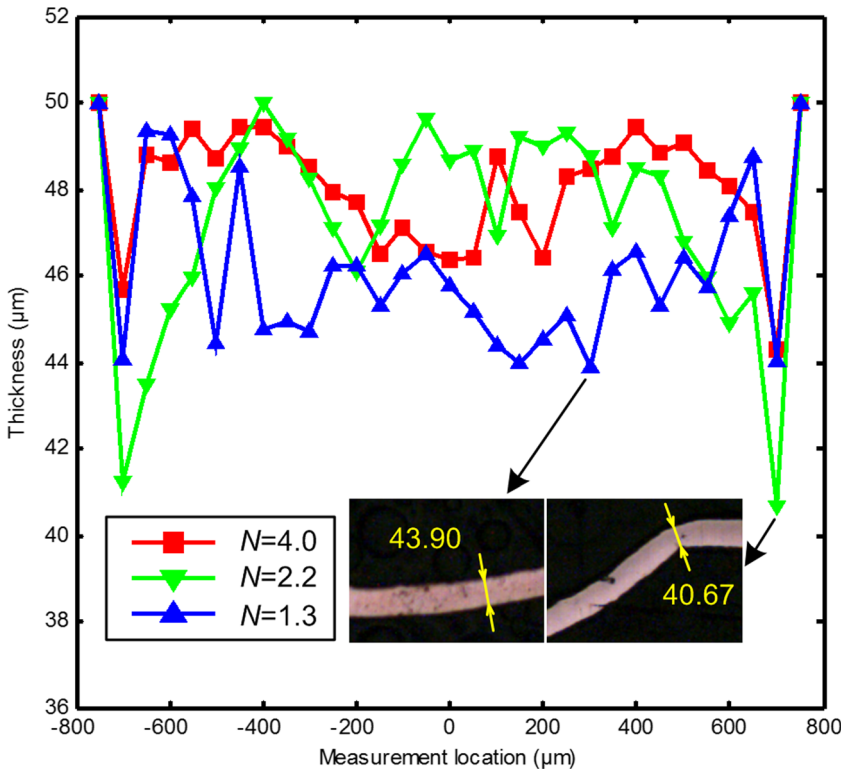

Fig. 8 Thickness distribution of bulged parts under laser power density of 2.63×10^{13} W/m^2

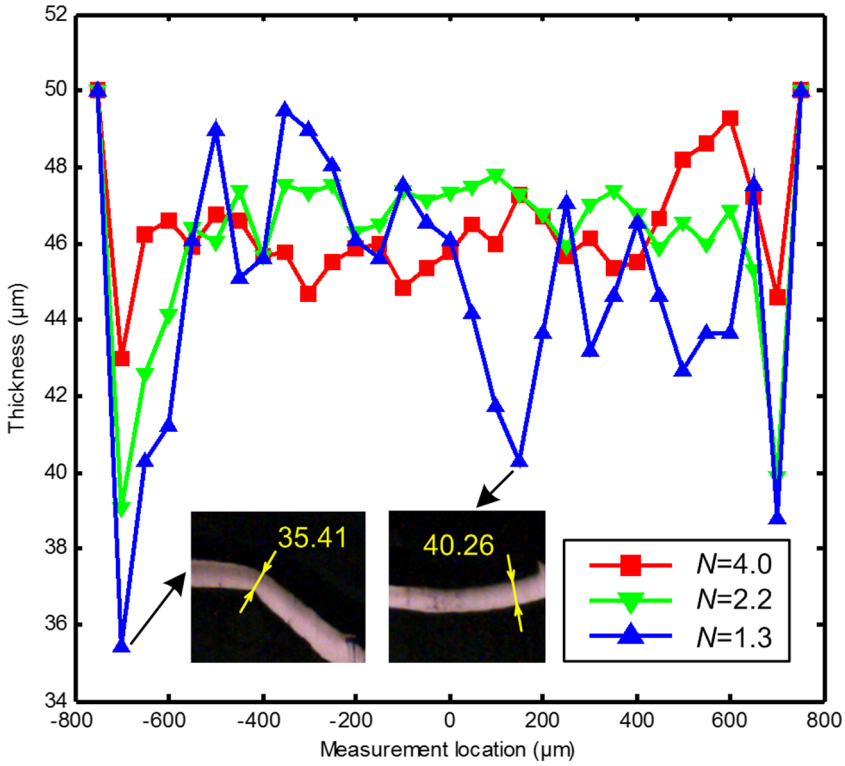

Fig. 9 Thickness distribution of bulged parts under laser power density of 3.51×10^{13} W/m^2

deformation in the cross section. It is observed that the high microhardness is mainly located at the fillet region of bulged parts in which the material undergoes the extensive plastic deformation. Moreover, the low microhardness is generally situated in the transition region since the corresponding material is drawn into the die and experiences less plastic deformation.

Figure 13 presents the microhardness distribution in the cross section of bulged parts with three N values under 3.51×10^{13} W/m^2. It is manifest that the similar distribution trend of microhardness is observed. However, the microhardness in the laser-shocked region does not increase accordingly with the enhancement of laser power density. In addition, the microhardness in the left fillet region is slightly higher than that in the right fillet. The nonuniform distribution of microhardness in the cross section implies that the size and distribution of grains strongly affect the plastic deformation of the metal foil.

Table 3 Maximum thickness thinning ratio with various grain sizes and laser power densities

N	Maximum thickness thinning ratio		
	2.63×10^{13} W/m^2 (%)	3.07×10^{13} W/m^2 (%)	3.51×10^{13} W/m^2 (%)
4.0	11	11	14
2.2	19	13	22
1.3	12	18	29

3.4 Surface morphology

It is well known that the surface quality is important for the performance of microparts. Thus, it is necessary to evaluate the initial grain size and laser power density effects on surface quality of laser shock bulged parts. Due to the difficulty of conducting roughness measurement on the dome-like shape part, the surface quality analysis is qualitatively studied in terms of surface morphology observation. Figure 14 shows the typical surface morphologies of bulged parts with three N values. It is observed that the bulged part surface tends to be rough with the increase of grain size. This result is consistent with the findings of microscale blanking and deep drawing compound process in quasi-static loading condition [20] and laser shock microbending forming of copper foil [24]. At $N = 4.0$, there are lots of grains located in the laser-shocked region, so the grains are easy to move along slipping systems leading to compatible and continuous strains between neighboring grains. Thus, the surface of bulged parts with fine grains can obtain good surface quality. However, as the grain size increases, the number of grains in the cross section is reduced. Compared with the inner grains, the surface grains suffer fewer constraints, and they are easier to move normally to the metal surface. This easily results in inhomogeneous plastic deformation and leads to the unsmooth surface. As a

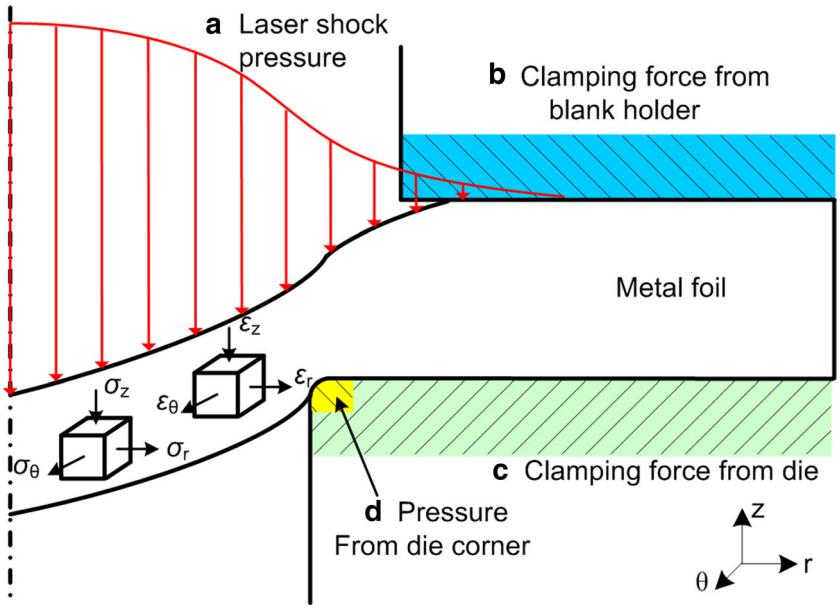

Fig. 10 Force acting during laser shock bulging process

consequence, it can be concluded that the grain size has a noticeable effect on the surface morphology of bulged parts.

Moreover, while the laser power density is enhanced from 2.63×10^{13} to 3.51×10^{13} W/m^2, the bulged part surface also seems to become rough, as shown in Fig. 14a, d. This phenomenon looks opposite to the conclusion reported by Wang et al. [24]. In the mentioned research, the surface morphology can be evidently improved by appropriately increasing laser power density. This difference results from the fact that the die structure of the present work is different from that in Wang et al. [24]. Herein, a die with through hole, i.e., without a bottom was applied.

3.5 Microstructure

Figures 15 and 16 show the typical microstructures of bulged parts with three N values under 2.63×10^{13} and 3.51×10^{13} W/m^2, respectively. Three regions are enlarged to show detail, denoted as A, B, and C. Regions A and C are related to the fillet region of the part, and region B correlates to the bottom zone. It can be seen that as the grain size increases, the grain size distribution of bulged parts becomes uneven, especially at $N = 1.3$. While the initial grain size is close to the foil thickness, there are only one or two grains in the cross section. Thus, single-crystal plastic deformation may occur

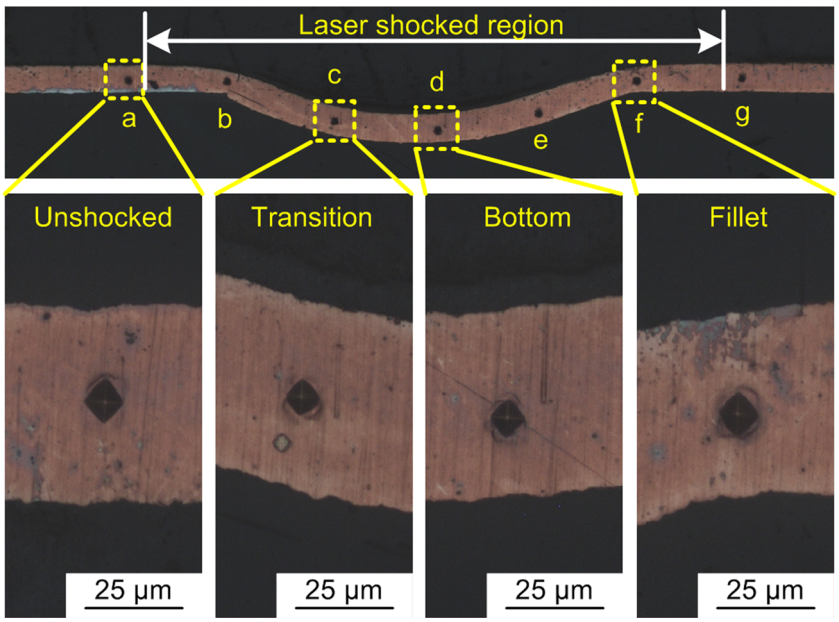

Fig. 11 Key microhardness measurements of bulged parts

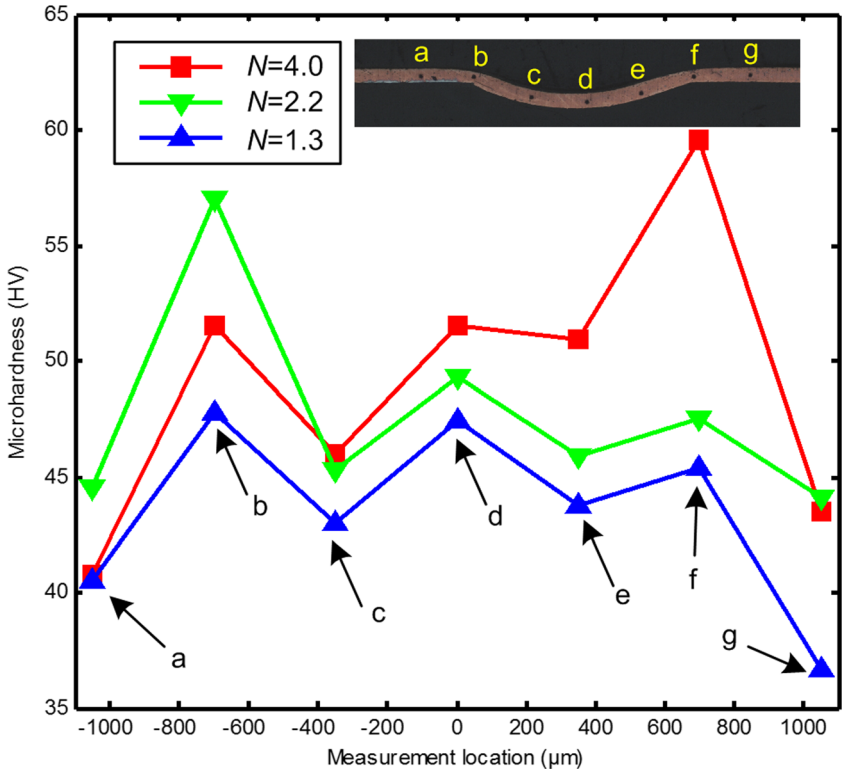

Fig. 12 Microhardness distribution of bulged parts under laser power density of 2.63×10^{13} W/m^2

and the mechanical properties of the individual grains will be dominant during the bulging process.

In order to further evaluate the change of microstructure subjected to laser shock loading, the grain size in the laser-shocked region, refer to Fig. 11, was measured by using the mean linear intercept method. Three specimens were tested in each condition. The comparison of average grain sizes with various grain sizes and laser power densities is given in

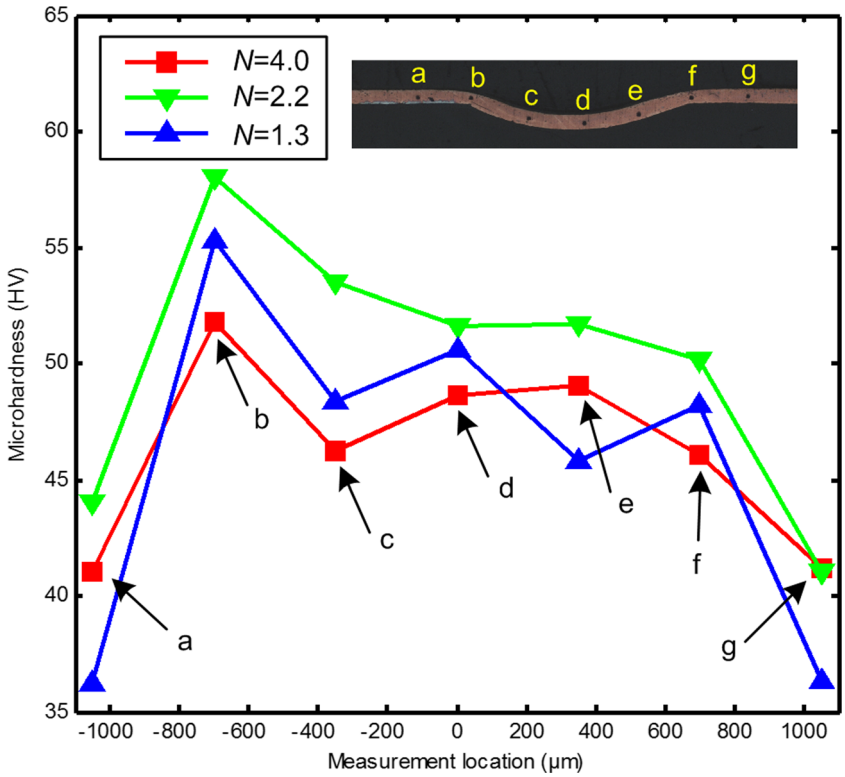

Fig. 13 Microhardness distribution of bulged parts under laser power density of 3.51×10^{13} W/m^2

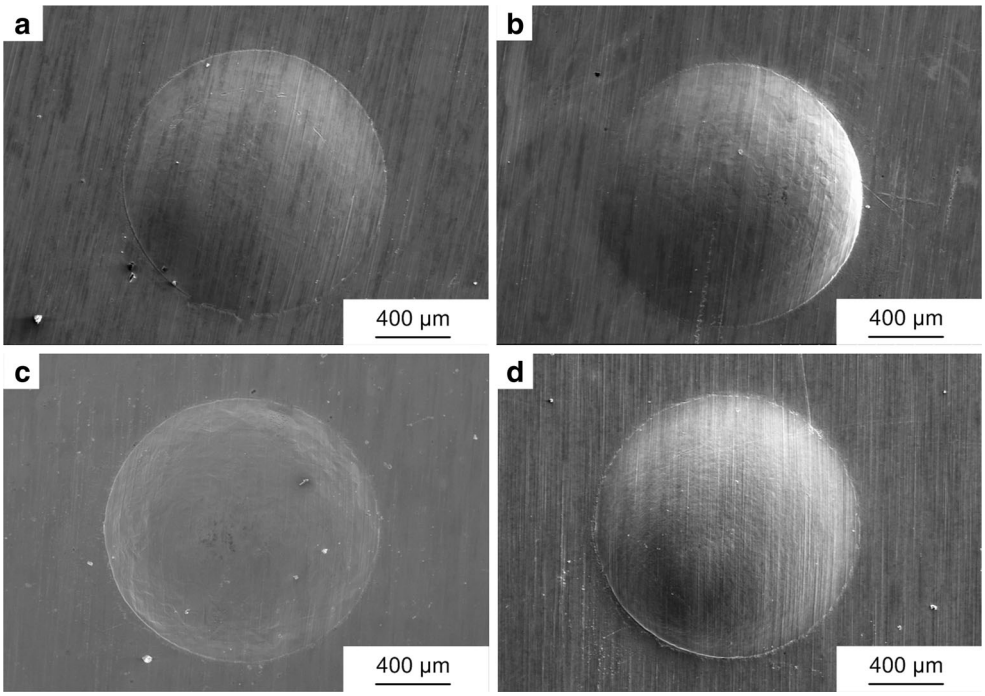

Fig. 14 Typical surface morphologies of bulged parts. **a** $N = 4.0$, 2.63×10^{13} W/m^2. **b** $N = 2.2$, 2.63×10^{13} W/m^2. **c** $N = 1.3$, 2.63×10^{13} W/m^2. **d** $N = 4.0$, 3.51×10^{13} W/m^2

Fig. 17. It can be manifestly seen that the grain sizes of bulged parts are slightly refined with the increase of laser power density. In addition, the grain refinement is more significant for the coarse-grained part, especially in the case of $N = 1.3$.

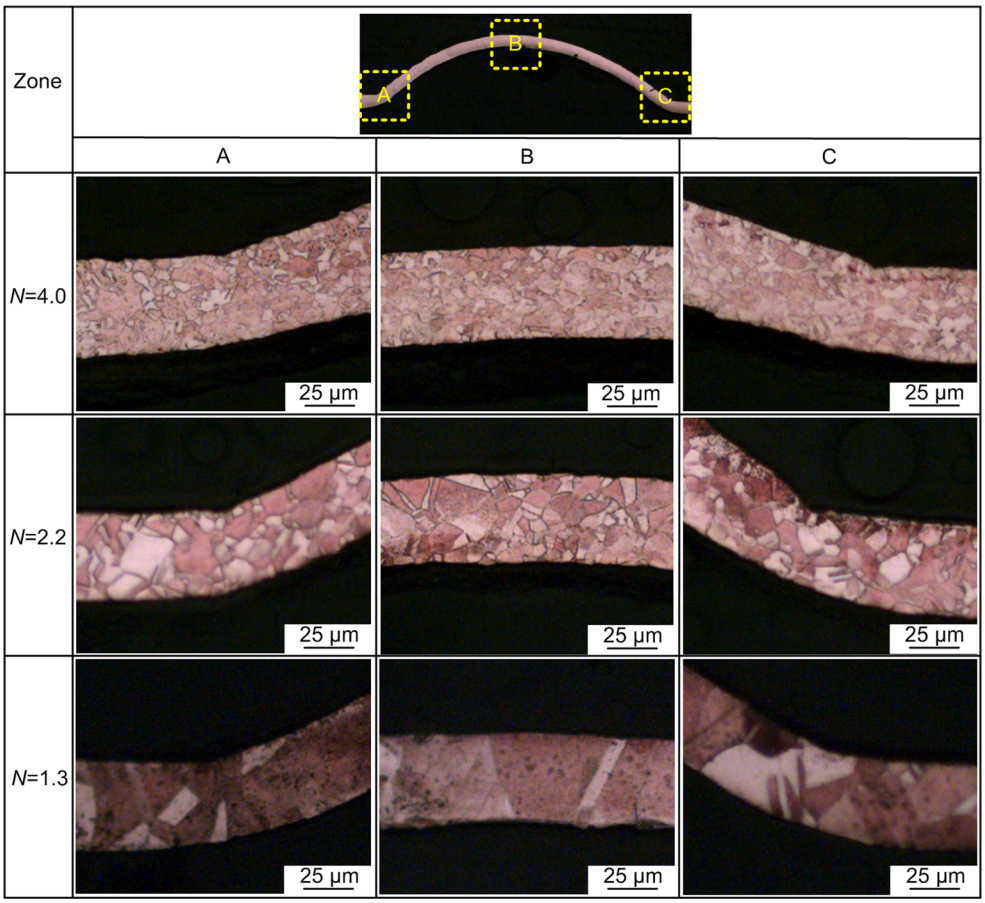

Fig. 15 Microstructures of bulged parts under laser power density of 2.63×10^{13} W/m^2

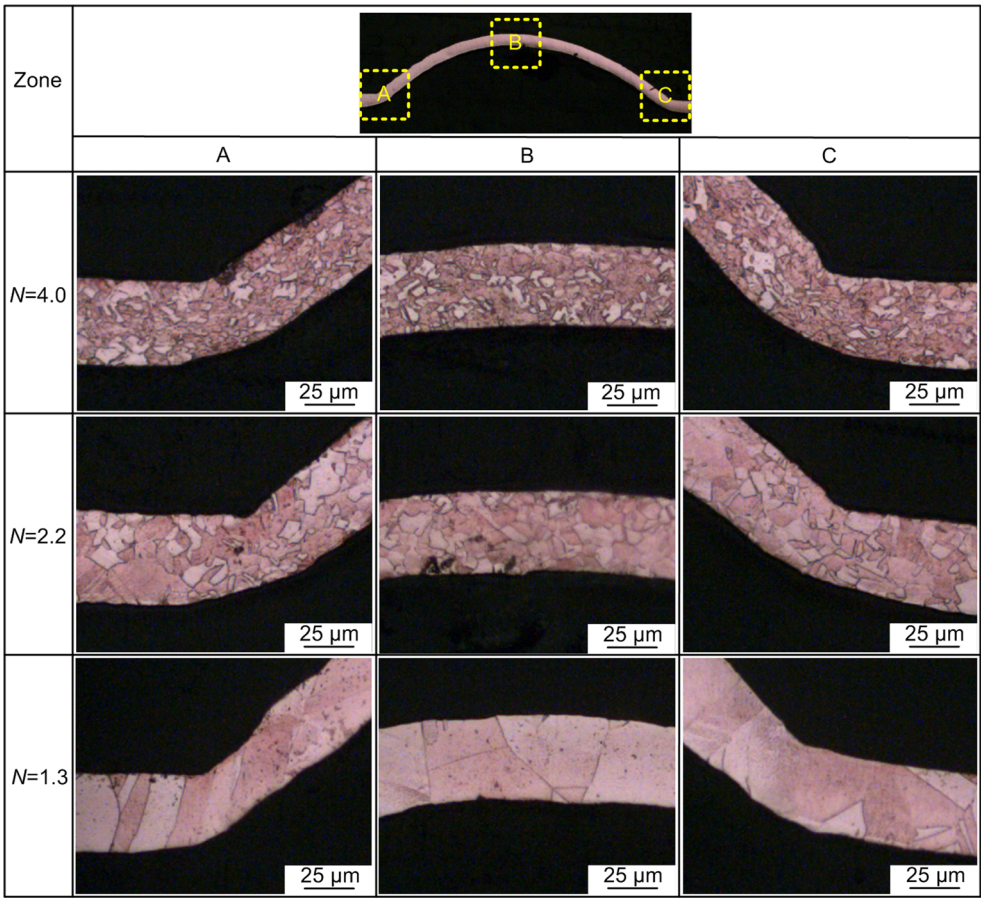

Fig. 16 Microstructures of bulged parts under laser power density of 3.51×10^{13} W/m^2

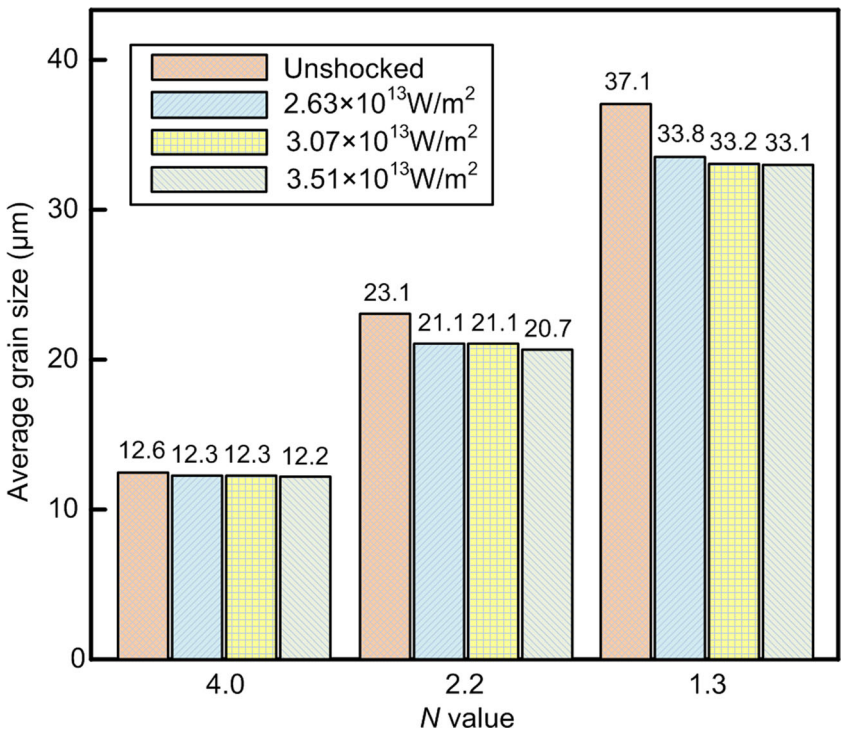

Fig. 17 Comparison of average grain sizes before and after laser shock bulging process

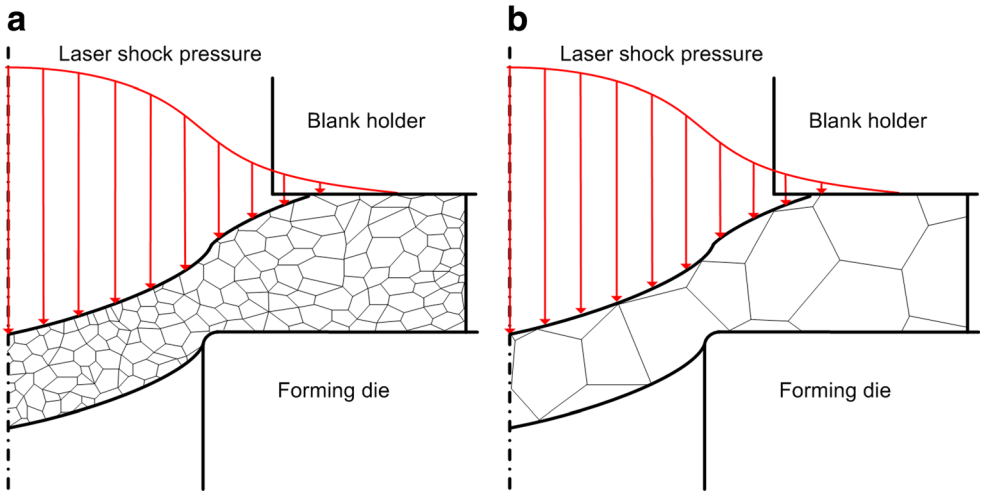

Fig. 18 Schematic illustration of the interactive effect of foil thickness and grain size. **a** $t > d$. **b** $t \approx d$

Obviously, the reduction of grain sizes brings about grain refinement strengthening, which is helpful for the performance of microparts.

The grain refinement phenomenon induced by high-power laser shock and its mechanism have attracted much attention in recent years. Lu et al. [32] revealed the microstructure features of the LY2 aluminum alloy during multiple laser shock processing. It is found that the microstructure has been evidently refined due to the ultrahigh plastic strains induced by multiple laser shock. They concluded that both large strains and high strain rates are necessary for the formation of refined grains during plastic deformation. Ye et al. [33] investigated the microstructure response of copper foil by femtosecond laser pulses. The experimental results show that the dislocation motion acts as the prevailing deformation modes in copper foil. According to Eq. (1), the generated laser shock wave pressure exceeds 4 GPa subjected to the applied laser power density. Under the ultrahigh pressure, the plastic deformation occurs at high strain rates due to the short laser-material interaction time. The bulging height can reach 160–340 μm in relation to the mechanical property of material and the laser power density, as shown in Fig. 5. At $N = 1.3$ and 3.51×10^{13} W/m^2, the thickness thinning ratio in the fillet region approaches 29%, refer to Table 3, indicating that the material of the corresponding region undergoes extensive plastic deformation during laser shock. Therefore, based upon the experimental results, the grain refinement in laser shock bulging forming process is attributed to the large plastic deformation at high strain rates under laser shock.

Based upon the above investigations, it can be found that the ratio N plays an important role in the forming quality of bulged parts. In order to illustrate the grain size effect on bulging process, a size effect model by considering the foil thickness and initial grain size was established, as shown in Fig. 18. When $t > d$, refer to N values of 4.0 and 2.2, there are lots of grains located in the laser-shocked region, which is helpful for slipping deformation. Therefore, the total plastic deformation can be shared by these fine grains, leading to relatively good forming quality. When $t \approx d$, refer to $N = 1.3$, there are several grains traversing through the foil thickness direction. The mechanical properties of the individual grains will be predominant during the bulging process, especially when there is only one grain located in the cross section. In this case, the plastic deformation of the metal foil is deeply affected by the location, size, and orientation of individual grains. This easily results in inhomogeneous plastic deformation compared with the material with fine grains, and is responsible for the nonuniform distribution of thickness and microhardness of bulged parts.

4 Conclusions

In this paper, the effects of initial grain size and laser power density on the forming quality of pure copper foil in laser shock bulging process were investigated. The characteristics of bulging height, thickness distribution, microhardness, surface morphology, and microstructure were examined. The following conclusions are drawn from this research:

(1) The bulging height increases as the grain size becomes large, and as the laser power density is enhanced for both fine and coarse grain foils. The exhibiting good formability of pure copper foil in laser shock bulging process is attributed to the inertial effect on necking stabilization and strain-rate effect on material constitutive behavior.
(2) The overall thickness of bulged parts decreases compared with its original thickness. The location of the thinnest position is mainly in the fillet region of parts, which is related to the stress and strain characteristics during bulging forming process.
(3) The microhardness in the laser-shocked region increases due to the strain hardening effect, but the microhardness distribution is nonuniform because

of the inhomogeneous plastic deformation. The microhardness of bulged parts does not increase significantly with the enhancement of laser power density.

(4) The bulged part surface tends to be rough with the increase of grain size and the enhancement of laser power density.

(5) The grain sizes of bulged parts are slightly refined with the increase of laser power density, especially for the coarse-grained part. The grain refinement in laser shock bulging forming process is attributed to the large plastic deformation at high strain rates under laser shock.

Funding information This work is supported by the National Natural Science Foundation of China (No. 51205232) and Natural Science Foundation of Shandong Province (No. ZR2017BEE006).

Compliance with ethical standards

Conflict of interest The authors declare that they have no conflict of interest.

References

1. Fu MW, Chan WL (2013) A review on the state-of-the-art microforming technologies. Int J Adv Manuf Technol 67(9–12): 2411–2437
2. Vollertsen F, Niehoff HS, Hu Z (2006) State of the art in micro forming. Int J Mach Tools Manuf 46(11):1172–1179
3. Zheng C, Sun S, Ji Z, Wang W, Liu J (2010) Numerical simulation and experimentation of micro scale laser bulge forming. Int J Mach Tools Manuf 50(12):1048–1056
4. Zhang XQ, Zhang Y, Yin YD, Zhang YW, Li SZ, Duan SW, Huang ZL, Chen B, Pei SB, Wang HT (2017) Simulation of the forming process of conical cup shaped by laser-induced shock waves. Int J Adv Manuf Technol 91(5–8):1619–1630
5. Liu HX, Sun XQ, Shen ZB, Li LY, Sha CF, Ma YJ, Gau JT, Wang X (2017) Experimental and numerical simulation investigation on laser flexible shock micro-bulging. Metals 7(3):93–108
6. Niehoff HS, Vollertsen F (2005) Non-thermal laser stretch-forming. Adv Mater Res 6-8:433–440
7. Vollertsen F, Niehoff HS, Wielage H (2009) On the acting pressure in laser deep drawing. Prod Eng 3(1):1–8
8. Zheng C, Sun S, Zhang GF, Song LB, Ji Z (2013) Effect of confining overlay in micro scale laser bulge forming. Appl Surf Sci 285: 477–482
9. Shen ZB, Liu HX, Wang X, Wang CT (2016) Improving the forming capability of laser dynamic forming by using rubber as a forming medium. Appl Surf Sci 369:288–298
10. Xu ZT, Peng LF, Fu MW, Lai XM (2015) Size effect affected formability of sheet metals in micro/meso scale plastic deformation: experiment and modeling. Int J Plast 68:34–54
11. Vollertsen F, Biermann D, Hansen HN, Jawahir IS, Kuzman K (2009) Size effects in manufacturing of metallic components. CIRP Ann Manuf Technol 58(2):566–587
12. Raulea LV, Goijaerts AM, Govaert LE, Baaijens FPT (2001) Size effects in the processing of thin metal sheets. J Mater Process Technol 115(1):44–48
13. Gau JT, Principe C, Yu M (2007) Springback behavior of brass in micro sheet forming. J Mater Process Technol 191(1–3):7–10
14. Kim GY, Koç M, Ni J (2008) Experimental and numerical investigations on microcoining of stainless steel 304. J Manuf Sci Eng Trans ASME 130(4):0410171–0410176
15. Justinger H, Hirt G (2009) Estimation of grain size and grain orientation influence in microforming processes by Taylor factor considerations. J Mater Process Technol 209(4):2111–2121
16. Hmida RB, Thibaud S, Gilbin A, Richard F (2013) Influence of the initial grain size in single point incremental forming process for thin sheets metal and microparts: experimental investigations. Mater Des 45:155–165
17. Ghassemali E, Tan MJ, Wah CB, Jarfors AEW, Lim SCV (2013) Grain size and workpiece dimension effects on material flow in an open-die micro-forging/extrusion process. Mater Sci Eng A 582:379–388
18. Wang JL, Fu MW, Ran JQ (2014) Analysis of size effect on flow-induced defect in micro-scaled forming process. Int J Adv Manuf Technol 73(9–12):1475–1484
19. Gao ZY, Peng LF, Yi PY, Lai XM (2015) Grain and geometry size effects on plastic deformation in roll-to-plate micro/meso-imprinting process. J Mater Process Technol 219:28–41
20. Fu MW, Yang B, Chan WL (2013) Experimental and simulation studies of micro blanking and deep drawing compound process using copper sheet. J Mater Process Technol 213(1):101–110
21. Xu J, Guo B, Wang CJ, Shan DB (2012) Blanking clearance and grain size effects on micro deformation behavior and fracture in micro-blanking of brass foil. Int J Mach Tools Manuf 60:27–34
22. Meng B, Fu MW, Fu CM, Wang JL (2015) Multivariable analysis of micro shearing process customized for progressive forming of micro-parts. Int J Mech Sci 93:191–203
23. Hu YX, Li KM, Qi CJ, Yao ZQ, Grandhi RV (2012) Size effect on indentation depth of oxygen-free high purity copper induced by laser shock processing. Trans Nonferrous Met Soc China 22: s573–s578
24. Wang X, Ma YJ, Shen ZB, Gu YX, Zhang D, Qiu TB, Liu HX (2015) Size effects on formability in microscale laser dynamic forming of copper foil. J Mater Process Technol 220:173–183
25. Zheng C, Sun S, Ji Z, Wang W (2010) Effect of laser energy on the deformation behavior in microscale laser bulge forming. Appl Surf Sci 257(5):1589–1595
26. Fabbro R, Fournier J, Ballard P, Devaux D, Virmont J (1990) Physical study of laser-produced plasma in confined geometry. J Appl Phys 68(2):775–784
27. Li FQ, Mo JH, Li JJ, Huang L, Zhou HY (2013) Formability of Ti-6Al-4V titanium alloy sheet in magnetic pulse bulging. Mater Des 52:337–344
28. Rohatgi A, Soulami A, Stephens EV, Davies RW, Smith MT (2014) An investigation of enhanced formability in AA5182-O Al during high-rate free-forming at room-temperature: quantification of deformation history. J Mater Process Technol 214(3):722–732
29. Neugebauer R, Bouzakis KD, Denkena B, Klocke F, Sterzing A, Tekkaya AE, Wertheim R (2011) Velocity effects in metal forming and machining processes. CIRP Ann Manuf Technol 60(2):627–650
30. Gao H, Cheng GJ (2010) Laser-induced high-strain-rate superplastic 3-D microforming of metallic thin films. J Microelectromech Syst 19(2):273–281
31. Cheng GJ, Pirzada D, Zhou M (2007) Microstructure and mechanical property characterizations of metal foil after microscale laser dynamic forming. J Appl Phys 101(6):063108–063114
32. Lu JZ, Luo KY, Zhang YK, Cui CY, Sun GF, Zhou JZ, Zhang L, You J, Chen KM, Zhong JW (2010) Grain refinement of LY2 aluminum alloy induced by ultra-high plastic strain during multiple laser shock processing impacts. Acta Mater 58(11):3984–3994
33. Ye YX, Feng YY, Lian ZC, Hua YQ (2014) Plastic deformation mechanism of polycrystalline copper foil shocked with femtosecond laser. Appl Surf Sci 309:240–249